Anisotropic Metal-Insulator Transition in Epitaxial Thin Films

I. B. Altfeder,[1,2] X. Liang,[2,3] T. Yamada,[4] D. M. Chen,[2] and V. Narayanamurti[1]

[1]*Division of Engineering and Applied Sciences, Harvard University, Cambridge, Massachusetts 02138, USA*
[2]*The Rowland Institute at Harvard, Cambridge, Massachusetts 02142, USA*
[3]*Institute of Physics, Chinese Academy of Sciences, Beijing, 100080, China*
[4]*NASA Ames Research Center, Moffett Field, California 94035, USA*

By comparing the properties of In and Pb quantum wells in a scanning tunneling microscopy subsurface imaging experiment, we found the existence of lateral bound states, a 2D Mott-Hubbard correlation gap, induced by transverse confinement. Its formation is attributed to spin or charge overscreening of quasi-2D excitations. The signature of the 2D confinement-deconfinement transition is also experimentally observed, with the correlation gap being pinned in the middle of the conduction band. A self-organized 2D Anderson lattice is suggested as a new ground state.

Quantum enhancement of strongly correlated phenomena represents an important motivation for the experimental study of nanostructures [1–3]. The evidence of unusual electronic localization in atomically flat thin Pb(111) films has previously been shown in scanning tunneling microscopy (STM) experiments [4–6]. A simple quasiclassical model was proposed for the explanation of this effect: owing to the nested hole Fermi surface of Pb, the electrons tunneling into these films move only in the direction of k quantization that causes the formation of quantum-dot-like (0D) states. An alternative picture, where the strong electronic anisotropy is *induced* by thin-film confinement, is of great interest and remains yet to be validated.

In principle, nonequilibrium 0D states may arise not only from material anisotropy, but also from the enhanced many-body interactions in a thin film, facilitated by finite-size and reduced dimensionality [2,7,8]. Indeed, considering these states as *electronic* impurities [9], i.e., artificial Anderson impurities, one would expect them to strongly interact with the electronic environment of a quantum well (QW). The existence of such correlations can be revealed by replacing Pb with another material, whose bulk Fermi surface is not nested in the direction of k quantization. Here, the development of electronic impurities would serve as experimental evidence that strong interactions indeed take place. A good candidate for this experiment would be a metal having one less p electron per atom than in Pb [10], as, for example, In [11,12]. For the STM experiment, a thin In film represents an interesting object for comparison for yet another reason: room-temperature deposition of both Pb and In on Si(111)(7 × 7) yields nanostructures of very similar geometry, i.e., (111)-oriented flattop islands with a face-centered cubic (fcc) lattice [13,14] (weakly distorted fcc for In [15]). Moreover, in both cases the 7 × 7 reconstruction is preserved under burial. Because of the geometric similarity of these nanostructures, the difference of their electronic properties will originate primarily from the difference of valence numbers (quasidoping effect) and Fermi surface topologies.

Here, we present an in-depth comparison of the electronic properties of thin Pb(111) and In(111) films. Our study suggests that thin epitaxial films of simple polyvalent metals represent a family of doped 2D Mott-Hubbard insulators, whose anisotropic transport behavior is most likely stabilized due to Coulomb interaction between localized and delocalized electronic states.

The experiments were performed in a dual-chamber UHV system equipped with surface preparation and analysis tools and with a low-temperature STM. A silicon substrate was cleaned by a sequence of flashing to 1100 °C and ion sputtering. After a clean 7 × 7 reconstructed Si(111) surface was obtained, metal atoms were deposited from an effusion cell with a rate of ~1 monolayer (ML)/ min to form an epitaxial film. The quality and the chemical composition of the surface both before and after deposition were monitored using reflective high-energy electron diffraction and Auger spectroscopy. The sample was then transferred *in situ* into the STM analysis chamber. During the measurements, the voltage was applied on the tip while the sample was grounded.

Figure 1 shows a typical STM image of In(111) film obtained at 77 K. Following the Stranski-Krastanov mode, flattop nanocrystals are grown on top of the In wetting layers. Careful analysis shows that the majority of islands are confined between the substrate steps, forming arrays oriented along the step edges. In Fig. 1, two of the arrays are indicated by dashed lines. This effect is probably caused by a diffusion barrier at a step edge, which confines deposited atoms within a single terrace. Anisotropic diffusion resulting from such a confinement may be responsible for elongated island geometry. The height distribution of *confined* (uniform thickness) islands is shown in Fig. 2(d). Forbidden and allowed values, clearly exhibited in the histogram, resemble the electronic growth earlier reported for thin Pb films [16,17].
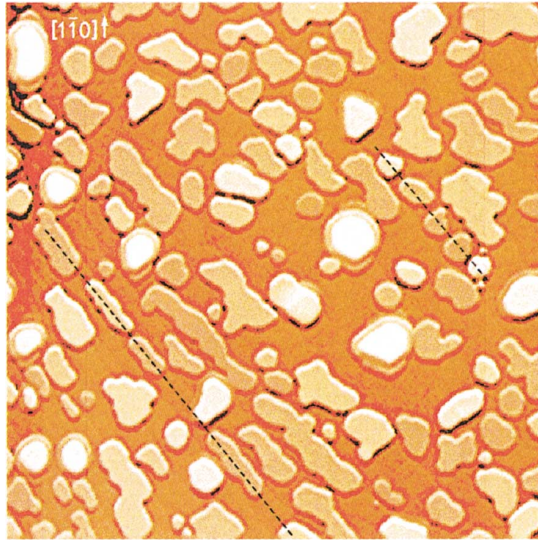
FIG. 1 (color).   A typical STM image of In islands on Si(111), obtained at $V = 0.5$ V, $I = 0.1$ nA. The image size is 1600×1600 nm^2.

FIG. 2.   (a) The density of states spectra for different In islands. (b) The dependence of Δ^{-1} on the number of atomic layers. (c) Spectral shift introduced by 1 ML thickness change in a wedge-shaped island. (d) Height distribution histogram for uniform thickness In(111) islands.

There, the appearance and the periodicity of "magic heights" is induced by $\lambda_F/2$ transverse modulation of charge density ($\lambda_F \approx 4a$; $a = 1$ ML). Likewise, we conclude (suggest) that for In(111) islands $\lambda_F \approx 8a$.

In Fig. 2(a), we show the tunnel density-of-states spectra, measured for different In islands. The spectra exhibit distinct resonant features, whose energy separation decreases with the increase of thickness. Such a behavior is expected for electron confinement in a one-dimensional quantum box, where quantized states E_n are separated by a gap $\Delta = \pi\hbar v/H$, with v being the electron velocity and H the film thickness. The modification of tunnel spectra with the decrease of metal height by 1 ML is illustrated in Fig. 2(c). As shown earlier [18], for electrons confined in a 1D quantum box the change of thickness by 1 ML introduces a spectral shift $\delta \approx \Delta(2a/\lambda_F)$. In the case of In(111) films, we found $\delta \approx \Delta/4$, again indicating that $\lambda_F \approx 8a$. The narrow, $\sum \approx 0.4$ eV, width of the 2D subbands indicates a large 2D effective mass, $M^* \gtrsim 20m_e$. The spectral data are summarized in Fig. 2(b), where we plot Δ^{-1} as a function of the number of atomic layers. The electron velocity perpendicular to the interface, as determined from Fig. 2(b), is $v_\perp \approx 2 \times 10^8$ cm/s. The thickness offset of the film, introduced by In wetting layers, may be responsible for the horizontal offset in Fig. 2(b).

Thus, the electrons confined in In(111) films oscillate between its opposite boundaries with a typical free-electron velocity, possessing at the same time large in-plane effective mass. The twofold increase of λ_F in In(111) films in comparison with Pb(111) films is most likely due to smaller electron density [larger volume of hole Fermi surface; see Fig. 3(g)].

Owing to transverse electronic oscillations, the STM images of In(111) islands reveal information about the buried In/Si(111) interface. In Figs. 3(a)–3(d), we show
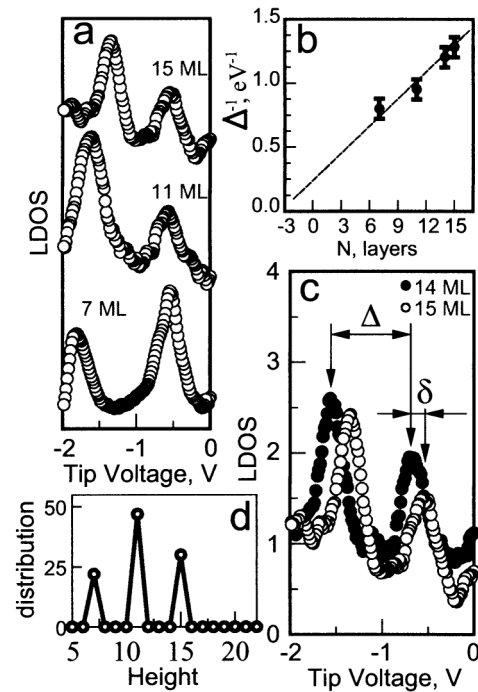
the sequence of voltage-dependent STM images obtained on top of a 7 ML (thickness $H = 9a$) island. Comparison of the images indicates partial preservation of the 7×7 reconstruction, accompanied by self-assembly of a nanoscale domain structure due to interfacial alloying. The bright defects, seen in Fig. 3(a) ($V_{tip} = 250$ mV), illustrate the "tops" of subsurface pyramid-shaped structures, created by alloying of Si and In atoms. The change of tunnel bias in Fig. 3(b) ($V_{tip} = -250$ mV) shifts the vertical position of the imaging plane $h = \pi n/k_\perp(E)$ closer to the interface. Now, the 7×7 reconstructed In/Si(111) interface becomes visible in the STM image, while the bright defects increase in size and transform into nanoscale islands. Further increase of the tunnel bias [Fig. 3(c), $V_{tip} = -450$ mV] enhances the contrast of the interfacial image, making the area occupied by islands even larger. In a situation of Fig. 3(c), the imaging plane coincides with the interface ($h = H$), and STM resolves the "bases" of three-dimensional interfacial structures, rather than their tops [seen in Fig. 3(a)]. The electronic image of the buried interface disappears in Fig. 3(d) due to off-resonance situation ($V_{tip} = -850$ mV).

Quite surprisingly, the structure of a buried In/Si(111) interface can be resolved in fine detail. The STM cross sections, shown in Fig. 3(f), suggest the lateral resolution $\xi \approx 0.7$ nm. Moreover, the STM images do not reveal any signature of lateral interference fringes around subsurface defects [19], whose formation is expected for coherent 3D Bloch waves. On the contrary, such an anisotropic
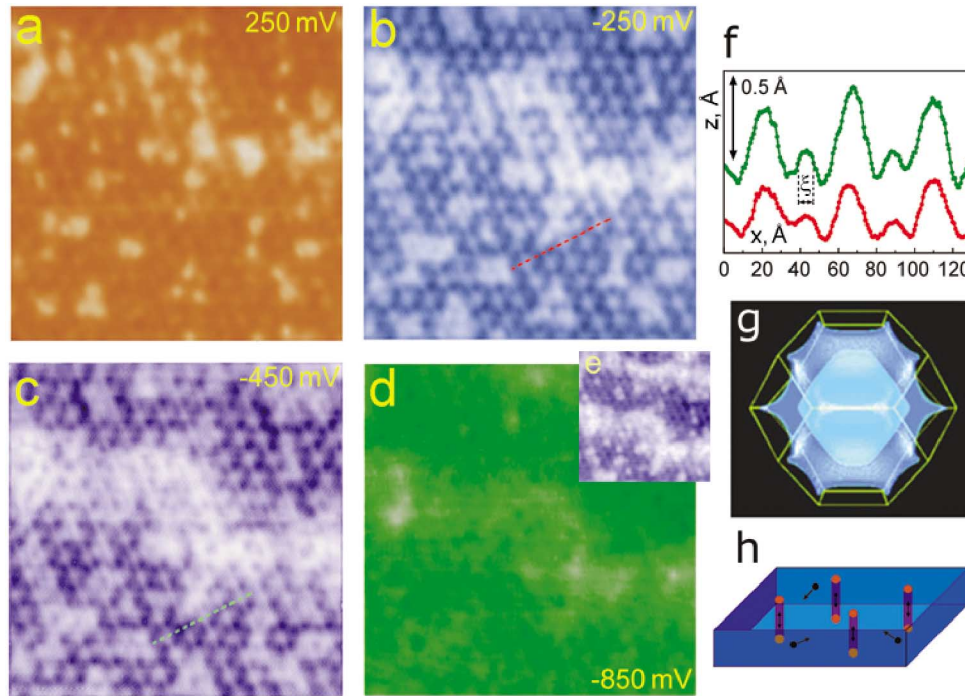
FIG. 3 (color). (a)–(d) The 400×400 Å^2 STM images of 7 ML island, obtained at different tip voltages: (a) $V = 250$ mV, (b) $V = -250$ mV, (c) $V = -450$ mV, (d) $V = -850$ mV; ($I = 0.2$ nA). (e) Reappearance of a resonant image at -3.4 V. (f) The cross sections of Figs. 3(b) and 3(c) where large and small peaks originate from subsurface corner holes and dimer dislocations. (g) Hole Fermi surfaces of In and Pb (inner). (h) Anisotropic excitations (vertical columns) and Fermi liquid quasiparticles.

one-dimensional character of interference would be typical for the array of incoherently coupled one-dimensional channels [20,21] ("electronic wires") oriented along the axis of k quantization [Fig. 3(h)]. As the bulk material does not exhibit a nested Fermi surface, their formation is likely to be caused by thin-film confinement.

The difference of electronic configurations of In and Pb islands manifests not only in the twofold change of λ_F. As we found from the analysis of broad energy range spectroscopic measurements, the change of electron density can be *directly* observed in tunnel spectra. In the upper inset of Fig. 4, we show the current-voltage characteristic of an In island. The resonant feature at -0.6 V is clearly resolved. Applying a large (>1 eV) tunnel bias significantly modifies the shape of a potential barrier, resulting in an exponential enhancement of the tunnel matrix elements and a strong I-V nonlinearity. This nonlinearity can be eliminated in the normalized I-V spectra, shown in Fig. 4, where the data were measured in a broad (± 4 V) range of tunnel bias and presented using a linear-logarithmic vertical scale arcsinh(I). In addition, in Fig. 4 we show the normalized I-V spectrum of a Pb(111) sample, probed in the same range of tunnel bias. Comparison of the curves shows that, while in Pb(111) films the quantum-dot-like interference abruptly vanishes when the energy of tunneling electrons exceeds 2.0–2.5 eV, in In(111) films such an interference persists to the very top of a potential well (with little $\sum_n$ dependence). In the same range of tunnel bias the resonant

behavior of STM images was observed [see Fig. 3(e)]. It seems natural to suggest that the rise in energy of resonances in In(111) films in comparison with Pb(111) films has to do with the reduction of the Fermi energy as a consequence of reduced electron density.

In the tight-binding model, electronic states near the middle of the conduction band (half-filling) form a quasi-1D gas with a linear dispersion $E(k) = \nu \hbar (k_{\perp} - \pi/2a)$. The next order quadratic terms are absent since in the middle of the band the effective masses become infinitely large. Confinement of these quasi-1D electrons in a finite-size potential well creates 0D states with nearly equidistant energy levels (E_n). In principle, moving away from the middle of the conduction band introduces a nonzero lateral bandwidth ($t_{\parallel}$). Following the argumentation of metal-insulator transition [22], the transformation of 0D states into 2D states occurs when $t_{\parallel} > U$, where U is the on-site "bound" energy. According to Fig. 4, quantum dot states develop inside a $2U \approx 4$–5 eV energy window, whose center is pinned in the middle of the conduction band. For a metal with almost half-filled band, such as Pb, this energy window is symmetric around the Fermi level, illustrated as (a) in the lower inset of Fig. 4. For In, whose conduction band is significantly less than half-filled, the energy window for 0D states becomes asymmetrically lifted with respect to the Fermi level, shown as (b) in the lower inset of Fig. 4. Since tunnel spectroscopy primarily detects unoccupied 0D states [23], only unoccupied portions of these energy windows
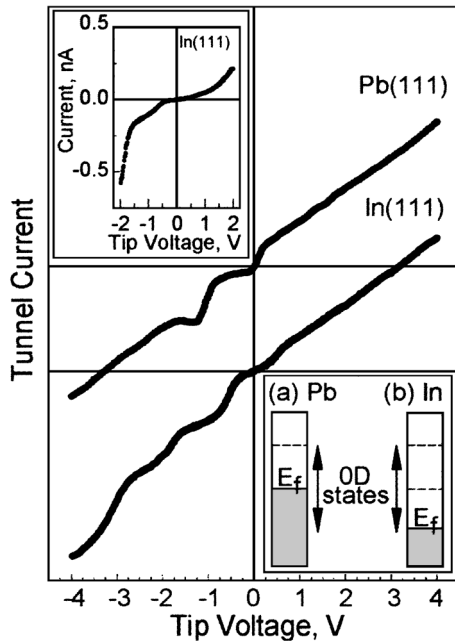
FIG. 4. Normalized tunnel *I-V* characteristics of In and Pb films, obtained in ± 4 V bias range. Upper inset: Tunnel *I-V* characteristic of In island in a bias range ± 2 V. Lower inset: The energy window of 0D states is pinned in the middle of the conduction band: (a) half-filled band, (b) less than half-filled band.

can be seen in our data in Fig. 4. Thus, due to the reduction of the electron density a part of the occupied resonant states has been lifted above the Fermi level.

A possible reason for the 2D anomalies observed in our samples, including (a) the appearance of large 2D effective mass, (b) the absence of lateral interference, and (c) the signature of 2D bound energy, could be the formation of 2D Anderson lattice due to Coulomb interaction between *localized* and *delocalized* states [24] [see Fig. 3(h)]. In a simplest description of this effect, the electrons sequentially injected into a QW become surrounded by a cloud of antiparallel spins. The correlation gap produced by this spin or charge geometry "confines" electrons at a given point of the (111) plane, apparently not affecting their ability to perform transverse ballistic oscillations (2D Kondo-like interaction). Through such a "confinement," coherent 2D Bloch waves transform into incoherent heavy electrons, shown in Fig. 3(h).

In conclusion, a surprising interplay between the transverse and the lateral electron confinement in a thin film, as discussed in this Letter, represents a clear example of quantum enhancement of Coulomb interaction [25]. This enhancement, unlike in previously known models, arises from the lack of a microscopic disorder, i.e., from the elastic electron reflections at atomically flat crystal boundaries. Indeed, in the absence of transverse confinement ($H = \infty$) the screening cloud is unable to follow the electron, and the lateral bound states do not form. In quasi-1D materials, where 2D confinement-

deconfinement transitions were studied before [22], the possibility of coherent pair hopping has been discussed. A similar possibility may exist in QW where the electronic wires self-organize in 2D lattices.

[1] O. Pietzsch *et al.*, Science **292**, 2053 (2001).
[2] D. J. Huang, G. Reisfeld, and M. Strongin, Phys. Rev. B **55**, R1977 (1997).
[3] B. G. Orr, H. M. Jaeger, and A. M. Goldman, Phys. Rev. Lett. **53**, 2046 (1984).
[4] I. B. Altfeder, V. Narayanamurti, and D. M. Chen, Phys. Rev. Lett. **88**, 206801 (2002).
[5] W. B. Su *et al.*, Phys. Rev. Lett. **86**, 5116 (2001).
[6] I. B. Altfeder, D. M. Chen, and K. A. Matveev, Phys. Rev. Lett. **80**, 4895 (1998).
[7] R. Egger and H. Grabert, Phys. Rev. Lett. **79**, 3463 (1997).
[8] J. van den Brink and G. A. Sawatzky, Europhys. Lett. **50**, 447 (2000).
[9] D. Goldhaber-Gordon *et al.*, Nature (London) **391**, 156 (1998).
[10] J. R. Anderson and A. V. Gold, Phys. Rev. **139**, A1459 (1965).
[11] N. W. Ashcroft and W. E. Lawrence, Phys. Rev. **175**, 938 (1968).
[12] J. Chowdhuri, P. Chatterjee, and S. Chatterjee, J. Phys. F **9**, 683 (1979).
[13] A. Pavlovska, E. Bauer, and M. Giessen, J. Vac. Sci. Technol. B **20**, 2478 (2002).
[14] S. L. Surnev, J. Kraft, and F. P. Netzer, J. Vac. Sci. Technol. A **13**, 1389 (1995).
[15] The 7%−8% tetragonal distortion. Earlier studies indicated that in thin films it reduces or disappears (Ref. [14] and references therein).
[16] M. Hupalo and M. C. Tringides, Phys. Rev. B **65**, 115406 (2002).
[17] R. Otero, A. L. Vázquez de Parga, and R. Miranda, Phys. Rev. B **66**, 115401 (2002).
[18] I. B. Altfeder, K. A. Matveev, and D. M. Chen, Phys. Rev. Lett. **78**, 2815 (1997).
[19] M. F. Crommie, C. P. Lutz, and D. M. Eigler, Nature (London) **363**, 524 (1993).
[20] P. W. Anderson, Phys. Rev. Lett. **67**, 3844 (1991).
[21] V. J. Emery *et al.*, Phys. Rev. Lett. **85**, 2160 (2000).
[22] V. Vescoli *et al.*, Science **281**, 1181 (1998).
[23] Manifestation of electron-hole asymmetry in tunneling: holes tunnel as electrons.
[24] Apparently, only the (111) segment of hole Fermi surface can be affected by localization.
[25] Although not for thin films, a transformation of a free-electron metal into an insulator has been discussed in theory: A. W. Overhauser, Phys. Rev. Lett. **4**, 462 (1960); A. W. Overhauser and L. L. Daemen , Phys. Rev. Lett. **61**, 1885 (1988).